

# RECLAMATION

*Managing Water in the West*

## **The Application of Light Detection and Ranging (LiDAR) Technology to Improve the Management and Protection of Heritage Assets in the American Falls Archaeological District, Idaho**

**Project ID: 9541**



**U.S. Department of the Interior  
Bureau of Reclamation  
Pacific Northwest Region  
Boise, Idaho**

**September 2012**

U.S. DEPARTMENT OF THE INTERIOR

Protecting America's Great Outdoors and Powering Our Future

The U.S. Department of the Interior protects America's natural resources and heritage, honors our cultures and tribal communities, and supplies the energy to power our future.

MISSION OF THE BUREAU OF RECLAMATION

The mission of the Bureau of Reclamation is to manage, develop, and protect water and related resources in an environmentally and economically sound manner in the interest of the American public.

# RECLAMATION

*Managing Water in the West*

## **The Application of Light Detection and Ranging (LiDAR) Technology to Improve the Management and Protection of Heritage Assets in the American Falls Archaeological District, Idaho**

**Project ID: 9541**

**Principal Investigator: Jennifer Huang, Archaeologist**



**U.S. Department of the Interior  
Bureau of Reclamation  
Pacific Northwest Region  
Boise, Idaho**

**September 2012**



# TABLE OF CONTENTS (CONTINUED)

---

Abstract .....	1
Introduction.....	1
Data Quality Assessment .....	2
LiDAR Data Error.....	2
Interpolation Error .....	4
Uncertainty Analysis in Multi-temporal Terrain Surface Comparison.....	5
Study Area .....	7
Data .....	7
Methods.....	8
Surface Models .....	8
Change Detection.....	9
Error Analysis .....	10
Results .....	10
Error Analysis .....	10
Change Detection Approaches.....	13
Discussion.....	28
References.....	29

## List of Tables

Table 1.	LiDAR point statistics for study datasets.....	8
Table 2.	Error assessment for data processed for change detection.....	10
Table 3.	Height difference values for Anselin Local Moran I Cluster types (mass point to TIN using inverse distance). .....	16
Table 4.	Height difference values for Anselin Local Moran I Cluster types (mass point to TIN using inverse distance squared).....	16
Table 5.	Height difference values for Anselin Local Moran I Cluster types (mass point to DTM using inverse distance). .....	16
Table 6.	Height difference values for Anselin Local Moran I Cluster types (mass point to DTM using inverse distance squared). .....	16
Table 7.	Height difference values for Anselin Local Moran I Cluster types (Lake Walcott, Tile 03). .....	27

## TABLE OF CONTENTS (CONTINUED)

---

Table 8.	Height difference values for Anselin Local Moran I Cluster types (Lake Walcott, Tile 05). .....	27
Table 9.	Height difference values for Anselin Local Moran I Cluster types (Lake Walcott, Tile 07). .....	27
Table 10.	Height difference values for Anselin Local Moran I Cluster types (Lake Walcott, Tile 10). .....	27
Table 11.	Frequency of Probable Error in Height Difference Values for Lake Walcott Tiles.....	28

### List of Figures

Figure 1.	Sources of error related to data collection and post-processing. ....	3
Figure 2.	Example of comparing temporally discrete LiDAR datasets. ....	6
Figure 3.	Application of range of uncertainty to surface elevation difference grid. ....	12
Figure 4.	Examples of change detection results for the years between 2009 and 2011: a) deposition of material changing the course of the channel; b) erosion of gravel bar; c) erosion of stream terrace/flood plain; d) height difference of vegetation; e) suggested decrease in canopy height due to LiDAR data classification and/or interpolation error. ....	14
Figure 5.	Pattern analysis (Anselin Local Moran I) of surface elevation difference values. ....	15
Figure 6.	Frequency distribution of height difference values for Anselin Local Moran I Cluster types.....	17
Figure 7.	Pattern analysis (Getis-Ord Gi) of surface elevation difference values.....	18
Figure 8.	Channel cross-section survey transects with 2009/2011 difference grid.....	19
Figure 9.	Line graph of channel cross sections at transect 1.....	20
Figure 10.	Line graph of channel cross sections at transect 2.....	21
Figure 11.	Line graph of channel cross sections at transect 3.....	21
Figure 12.	Line graph of channel cross sections at transect 4.....	21
Figure 13.	Line graph of channel cross sections at transect 5.....	22
Figure 14.	Line graph of channel cross sections at transect 6.....	22
Figure 15.	Line graph of channel cross section at transect 7. ....	22
Figure 16.	Line graph of channel cross section at transect 8. ....	23

## TABLE OF CONTENTS (CONTINUED)

---

Figure 17.	Line graph of channel cross section at transect 9. ....	23
Figure 18.	Line graph of channel cross section at transect 10. ....	23
Figure 19.	Line graph of channel cross section at transect 11. ....	24
Figure 20.	Line graph of channel cross section at transect 12. ....	24
Figure 21.	Line graph of channel cross section at transect 13. ....	24
Figure 22.	Line graph of channel cross section at transect 14. ....	25
Figure 23.	Line graph of channel cross section at transect 15. ....	25
Figure 24.	Channel profile survey transects with Getis-Ord Gi* results for 2009 points and 2011 1-foot DTM. ....	26

## TABLE OF CONTENTS (CONTINUED)

---

# THE APPLICATION OF LIGHT DETECTION AND RANGING (LIDAR) TECHNOLOGY TO IMPROVE THE MANAGEMENT AND PROTECTION OF HERITAGE ASSETS IN THE AMERICAN FALLS ARCHAEOLOGICAL DISTRICT, IDAHO

## Abstract

Change detection using LiDAR data was explored as a tool for monitoring the effects of land surface disturbances that may impact historically significant cultural resource sites. Error associated with LiDAR data collection and processing is identified as a key contributing component in raising uncertainty in change detection results. The traditional approach of digital change detection using continuous surfaces (i.e., imagery or raster datasets) was found to be problematic when applied to digital terrain models (DTMs). A methodology of using Anselin Local Moran I and Getis-Ord  $G_i^*$  to identify statistically significant patterns of temporal changes in elevation is introduced. Elevation values are transferred between temporally discrete datasets (i.e., from a surface model to mass points) to calculate height difference. Significant clusters of high or low values and outliers are identified by assessing each height difference values within the context of neighboring values. Cluster analysis and mapping differentiated spatial pattern associated with geomorphic processes from random distributions of height difference values. The methodology shows promise for identifying surface disturbances that may impact cultural resource sites and is generally applicable in detecting geomorphic change on the Earth's surface.

## Introduction

Archaeological sites within the American Falls Archaeological District are significant both individually and as an assemblage, with the District listed on the National Register of Historic Places (NHRP). Within the boundaries of the District in southeastern Idaho, which is located adjacent to a stretch of the Snake River below American Falls Dam, sandy soils and dune conditions dominate the landscape. They are especially vulnerable to surface impacts such as wind and water erosion, cattle trampling, and off-road vehicle use. All of these impacts have been identified as major factors threatening surface and sub-surface archaeological deposits. Erosion can greatly reduce a site's integrity and eventually eliminate the characteristics for which it has been identified as significant. Federal agencies, through several laws including the National Historic Preservation Act, are tasked with protecting and preserving significant cultural resources. It is necessary for Reclamation to gain understanding of the surface changes that are occurring within the American Falls Archaeological District so that appropriate actions can be taken to ensure the preservation of existing cultural resource sites.

Change detection using LiDAR data, collected with airborne sensors, is a potential tool for monitoring effects of surface disturbance that may impact cultural resource sites. The process of LiDAR-based change detection involves comparing ground elevation values of multi-temporal datasets. Whereas resulting values may be indicative of either removal or deposition of surface material, interpretation, and validation of change relies on understanding source data quality (e.g., vertical accuracy and surface representation).

## **Data Quality Assessment**

### **LiDAR Data Error**

Accuracy uncertainty in airborne LiDAR data, similar to other remotely sensed data, originates from both data collection and post-processing. One source of error arises from accounting for sensor location and orientation during data collection. Incorrect parameters for the pulse trajectory and global positioning system (GPS) calibration at the sensor can impact the calculation of geographic coordinates  $x$ ,  $y$ ,  $z$  at the point where the LiDAR was reflected from the Earth's surface. This type of error is mitigated, though not eliminated, with on-board instrumentation to measure aircraft attitude and GPS base stations to collect Real Time Kinematic (RTK) control. The RTK control is typically used to detect vertical error but is generally inadequate to assess radial accuracy of the  $x$ -,  $y$ -coordinates, particularly in complex terrain where horizontal error is most likely to affect vertical accuracy. Error is also introduced in post-processing the data when separating the point cloud into terrain and non-terrain points. Misclassification of points leads to errors of commission and omission. Errors of omission incorrectly identify terrain points as non-terrain points and are eliminated from being used to model the terrain surface. An error of commission misidentifies a non-terrain point as a terrain. Incorporation of these non-terrain points over-estimates elevation in the terrain surface model. Additional error is associated with land cover. Tall, dense vegetation may prevent the laser pulse from reaching the ground surface entirely. In the process of classifying terrain points, this has the effect of reducing localized point spacing to the point of producing large data voids. The total combination of errors within a LiDAR data product contributes to misrepresentation of the actual terrain surface (Figure 1).

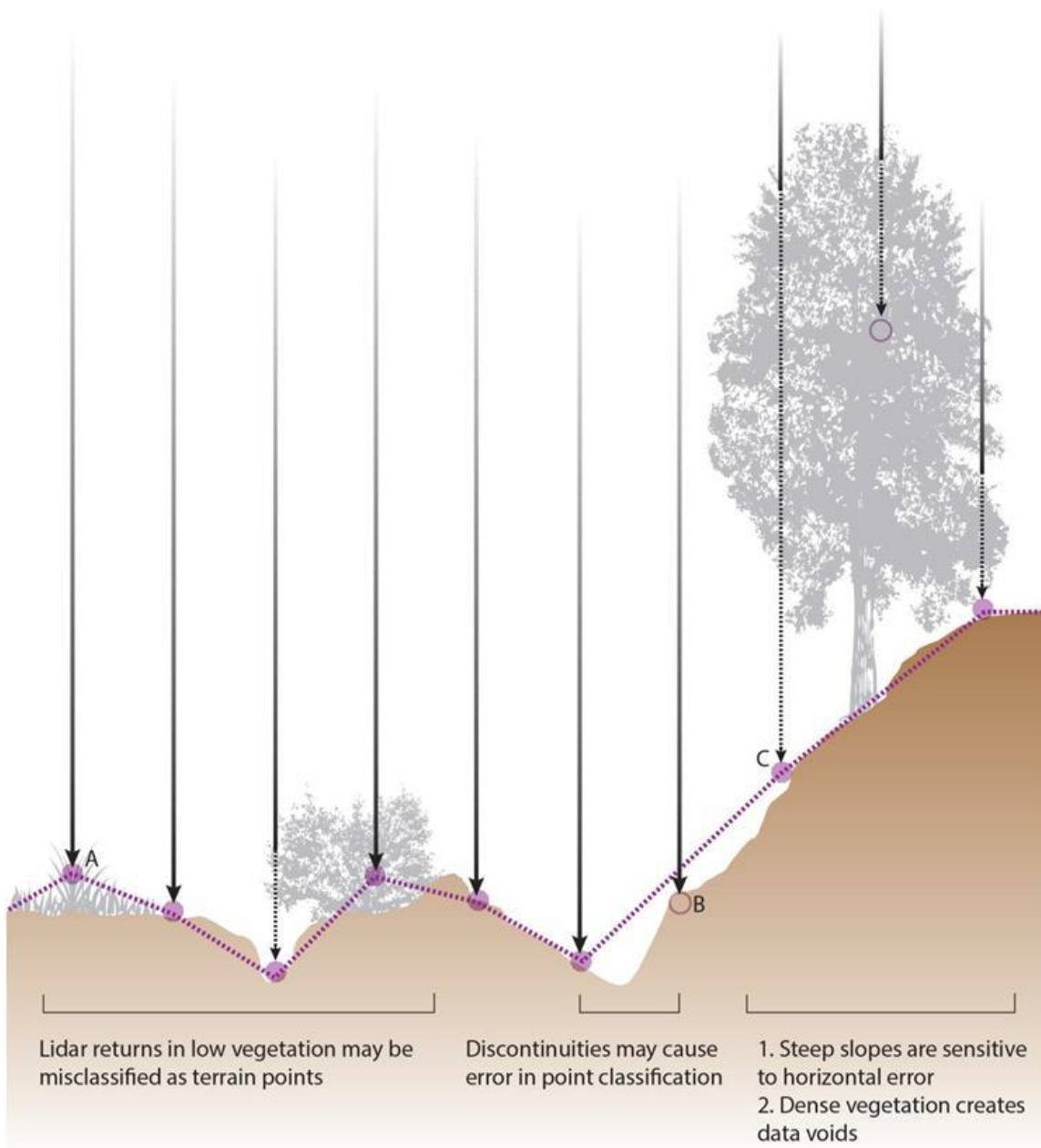


**Figure 1. Sources of error related to data collection and post-processing.**

Vertical accuracy is the principal criterion in specifying the quality of elevation data (ASPRS 2004). Commercial data providers manage and control data quality over the course of data collection and post-processing according to specifications prescribed by the end user. Reports typically included with the data products provide details on data collection, instrumentation, and accuracy assessment. To assess for vertical accuracy, acquired laser points are tested against GPS ground survey points. Industry-recognized standards substantiate vertical accuracy assessment in open terrain as fundamental; GPS ground survey is conducted in areas of open terrain (ASPRS 2004). Supplemental (i.e., optional) assessment may include a GPS ground survey more widely distributed throughout the dataset and stratified by common land cover types. Vertical error is reported as the deviation of the z-coordinate values between nearest laser points and ground survey points. Vertical error is reported as the root mean square error ( $RMSE_{(z)}$ ) of the elevation in terms of feet or meters (FGDC 1998). If vertical error is normally distributed, the linear error (vertical accuracy in ground distance) of the LiDAR dataset at the 95 percent confidence level is:  $Accuracy_{(z)} = 1.965 * RMSE_{(z)}$ . Reported accuracy values reflect uncertainty including those introduced by geodetic control coordinates, compilation, and final computation of surface coordinate values (ASPRS 2004). The reported statistical error and accuracy applies to terrestrial surfaces consistent with the level of GPS ground survey (i.e., fundamental or supplemental).

## Interpolation Error

Bare-earth LiDAR data points (i.e., mass points) must be interpolated to create a continuous terrain surface model, as either a Triangulated Irregular Network (TIN) or gridded DTM. Various interpolation methods exist and results may vary between each, implying a certain degree of error in interpolating elevation values and generating a surface model. The introduction of error in the process of interpolating data points is reported to be second to error generated during data collection and post-processing (Hodgson and Bresnahan 2004). Nominal post-spacing (i.e., sample density), terrain morphology, and vegetation impact interpolation results (Raber et al. 2002; Hodgson and Bresnahan 2004; Aguilar et al. 2005; Aguilar et al. 2010; Guo et al. 2010). These factors may be more decisive for DTM quality than the interpolation process itself (Cebecauer et al. 2002; Cvijetinovic et al. 2011). Nevertheless, kriging has been found to provide more accurate predictions than inverse distance weighted (IDW), natural neighbor (NN), regularized spline with tension (RST) or TIN interpolation methods (Guo et al. 2010; Gally et al. 2012).

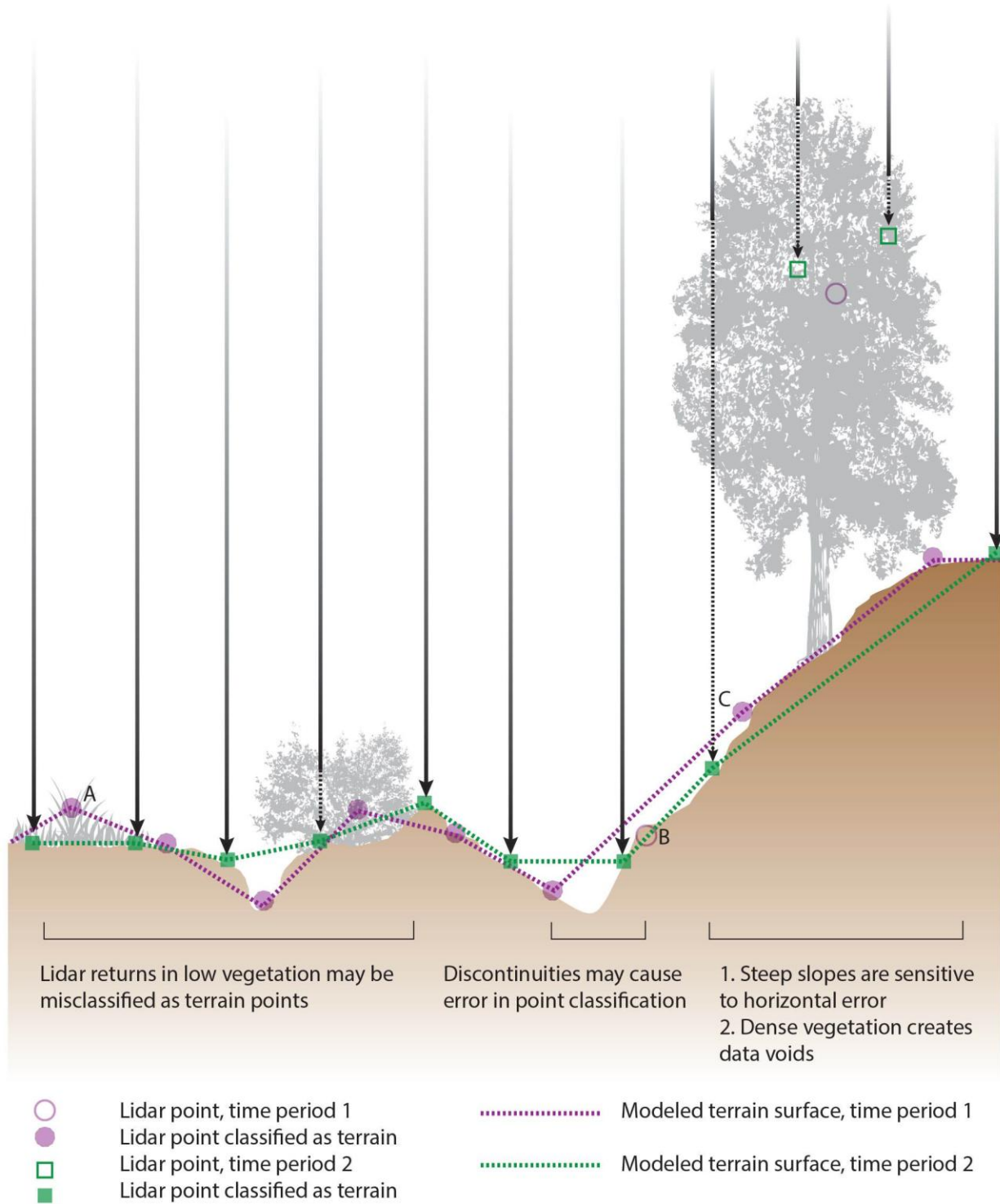
Cross-validation is an objective method to estimate and report geometric error and assess the accuracy of DTMs generated through interpolation methods (McGwire 1996). The cross-validation removes a control point from the dataset, the remaining data are processed, and the difference between the control point and processed data is calculated. The process is performed iteratively until all control points have been tested. A cross-validation RMSE is calculated. An alternative method, the ten-fold cross-validation, withholds a subset of the data points and the remaining data are used to estimate elevation values at the withheld

points (Kohavi 1995; Guo et al. 2010). Rather than incorporating a set of control points in the set of bare-earth data points, the dataset is randomly divided into 10 subsets. One subset is used as the validation set and the other subsets are used to interpolate an estimated surface. The process is repeated until all subsets have been used as a validation set. Estimated and actual elevation values at the location of the withheld points are assessed and RMSE is calculated to describe interpolation error.

## **Uncertainty Analysis in Multi-temporal Terrain Surface Comparison**

Change detection using LiDAR data involves quantifying differences in elevation between temporally discrete datasets at coincident points or overlapping cells. Elevation differences may be inferred to represent various types of surface disturbance and used to calculate degree or magnitude of change. The reliability of assertions and calculations lays in the accuracy of each dataset and is compounded in combining independent datasets. Dataset accuracy, reported as a global or stratified average, provides the range of values within which uncertainty exists as to whether surface values represent the actual surface. Total error further generalizes error between independent datasets.

Figure 2 displays potential error that may arise when the same terrain is sampled over two independent data collection efforts. LiDAR elevation samples are random as opposed to repeated in terms of the surface point that is sampled in each effort. Post-spacing (i.e., sampling density) is a critical factor influencing the accuracy of interpolated surfaces in terms of surface representation. This becomes more critical in managing range of variability when comparing two independent surfaces.



A - Error of commission, B - Error of omission, C - Horizontal displacement/error

**Figure 2. Example of comparing temporally discrete LiDAR datasets.**

An objective approach is required to quantify bounding limits distinguishing areas of measured change from error introduced through data collection, post-processing, and interpolation. The error in the LiDAR-derived surface models used to detect topographic change is a combination of vertical error ( $RMSE_{(z)}$ ) and interpolation error ( $RMSE_{(interpolation)}$ ). Surface error for each can be calculated as the RMSE of the sum of independent errors:

$$\text{Equation 1} \quad RMSE_{(surface)} = \sqrt{RMSE_{(z)}^2 + RMSE_{(interpolation)}^2}$$

The error of each surface ( $RMSE_{(surface)}$ ) is an independent error when calculating the difference in elevation between the surfaces. Thus, the total bounding error limit of uncertainty ( $RMSE_{(total)}$ ) is:

$$\text{Equation 2} \quad RMSE_{(total)} = \sqrt{RMSE_{(surfaceA)}^2 + RMSE_{(surfaceB)}^2}$$

Total error in this case is the accounting of vertical error (as reported by data providers) and calculated interpolation error. Other error may exist in the datasets that is not fully accounted for in the above equations.

## Study Area

A 17.4-acre (7 hectare) site in Union County, Oregon was selected as a test case for change detection of erosion and depositional processes. Multi-temporal, high-resolution LiDAR data was available and streamflow related surface disturbance was known to have occurred on the site. The northern third of the study area is dominated by agricultural land use and the lower third is comprised of natural and managed grassland. The agricultural and grassland areas are separated by Catherine Creek. A second site for which multi-temporal LiDAR data are available is located near Lake Walcott in eastern Idaho. This second study area is composed of primarily semi-arid shrub and grasslands with scattered agricultural use. The Snake River flows through the study area and American Falls is situated at the downstream extent of the study area. Streambank conditions are influenced by reservoir management/operations, upland areas are influenced by wind erosion, and recreational use occurs throughout the area, including watercraft and off-road vehicles.

## Data

LiDAR data collected in 2009 and in 2011 for portions of Catherine Creek in Union County, Oregon provide example data for assessing the feasibility of techniques to detect changes in the landscape that may impact archeological sites. High streamflow in the spring of 2010 and 2011 caused changes in stream channel and gravel bar location. This movement of unconsolidated surface material represents processes of erosion and deposition that occur within the American Falls Archeological District that could impact cultural assets. For the purpose of proof concept, subsets of the full datasets are used that

include sites of known geomorphic change within comparatively undisturbed areas. Average post-spacing was calculated for the 2009 and 2011 data subsets using point statistics (Table 1). Vertical error for the 2009 and 2011 datasets was calculated by the data provider and is assumed for the subsets.

LiDAR data were collected in 2003 and in 2011 within the vicinity of Lake Walcott Lake in Minidoka County, Idaho. Though changes in the land surface or land cover may have occurred, the purpose of the data collection was not for change detection; the data were collected to support other project work within the area. The fact that the data is representative of conditions typical of the American Falls Archaeological District makes them useful for exploratory analysis. Post-spacing was calculated and vertical error reported as with the Catherine Creek datasets (Table 1).

**Table 1. LiDAR point statistics for study datasets.**

Site	Acquisition Year	Post-spacing	RMSE <sub>z</sub>
Catherine Creek	2009	2.23 feet (0.68 meters)	0.09 feet (0.03 meters)
Catherine Creek	2011	1.42 feet (0.43 meters)	0.07 feet (0.02 meters)
Lake Walcott	2003	7.5 feet (2.28 meters)	0.09 feet (0.03 meters)
Lake Walcott	2011	3.34 feet (1.02 meters)	0.13 feet (0.04 meters)

## Methods

Two approaches of change detection are investigated using the LiDAR datasets collected for the Catherine Creek study area in 2009 and 2011. The first approach compares ground elevation values between two continuous surfaces modeled as grid-format DTMs. The second approach compares ground elevation values within the LiDAR point dataset against two interpolated surfaces, DTM and TIN models. This second approach was used in performing change detection between the 2003 and 2011 Lake Walcott datasets, using a point dataset against a TIN for comparing elevation between the two time periods.

Error analysis is performed to quantify error for each interpolation method. Combining error associated to LiDAR data collection and post-processing with error associated to data interpolation provides basis for assessing uncertainty in change detection results.

## Surface Models

Comparison of two raster surface models requires that each is of the same resolution. For comparison of continuous surfaces modeled from the 2009 and 2011 Catherine Creek LiDAR datasets, a resolution of 2 feet was used. This assumes less interpolation error when applying lower resolution to the relatively high-density 2011 point dataset than

applying high resolution to the lower density 2009 point dataset. These 2009 and 2011 LiDAR datasets were interpolated to continuous surfaces using ordinary kriging.

The point dataset to continuous surface comparison approach allows optimization of surface model resolution. The resolutions of the point dataset and continuous surface are not interdependent. The higher density point dataset can be used for interpolating the continuous surface and the lower density point dataset can be used to sample surface height difference. The 2011 Catherine Creek LiDAR dataset was interpolated using ordinary kriging at a resolution of 1 foot. For comparison of interpolation technique, the 2011 Catherine Creek LiDAR dataset was also interpolated to a TIN, inheriting the dataset post-spacing. The 2009 Catherine Creek LiDAR dataset required no processing in terms of interpolation.

In applying the mass point-to-surface model approach to the Lake Walcott datasets, the 2011 dataset was processed as a TIN and elevation values were transferred to the 2003 point data set for height difference calculations.

## **Change Detection**

A comparison of spatially coincident interpolated surface values was made between the 2009 and 2011 Catherine Creek DTMs using simple map algebra. Values in the 2009 DTM were subtracted from values in 2011 DTM to calculate change in the surface elevation values. The comparison of values between a continuous surface (i.e., DTM or TIN) and mass points was accomplished by transferring elevation information from the surface to the attribute table of the point dataset co-located to the specific point x-, y-coordinates. ArcGIS function “Extract Values to Points” was used to extract cell values from the 2011 DTM to the 2009 point datasets and “Add Surface Information” was used to transfer surface elevation information from the 2011 TIN to the 2009 point dataset. Subtraction of the 2009 surface values from the 2011 surface values was performed in the point dataset attribute tables to calculate change in surface elevation.

The use of point datasets for change detect affords the opportunity to apply spatial statistics and test for spatial autocorrelation of the calculated surface height differences. Both Anselin Local Moran I and Getis-Ord  $G_i^*$  statistics were used. These two statistics were applied in ArcGIS. Both inverse distance and inverse distance squared were used for conceptualization of spatial relationship in each of the statistics.

Change detection results were against assessed aerial imagery acquired concurrently with the acquisition of the LiDAR data. Visual inspection of the aerial imagery in areas identified as exhibiting significant change in the Catherine Creek study area was used to interpret and validate results. Stream transect survey data collected for Catherine Creek in 2011 was used to quantifiably compare survey data against transects replicated from the DTMs. Surface changes identified in the Lake Walcott datasets were assessed against aerial imagery acquired concurrently with the acquisition of the LiDAR data. Unlike the

Catherine Creek Study, there was no prior knowledge of surface disturbances that may have occurred in the area. The 2003 and 2011 imagery was visually inspected for sites of readily apparent change.

## Error Analysis

Ten-fold cross validation was performed to calculate interpolation error for the 2009 and 2011 DTMs and the 2011 TIN. Surface error was calculated for each surface following equation 1. Total error for surfaces with combined values through map algebra was calculated following equation 2. Error analysis was not performed for the Lake Walcott datasets.

## Results

### Error Analysis

Calculated total error was highest when both point datasets were interpolated into continuous surfaces and as DTM resolution differed from post-spacing (Table 2). Maximum difference in total error between change detection datasets was approximately 0.10 feet (0.03 meters); equivalent to 1.2 inches (0.3 centimeters).

**Table 2. Error assessment for data processed for change detection.**

DTM (2-foot, 2009)		DTM (2-foot, 2011)		Total Error	
RMSE <sub>z</sub>	0.09 ft (0.03 m)	RMSE <sub>z</sub>	0.07 ft (0.02 m)		
RMSE <sub>interpolation</sub>	0.17 ft (0.05 m)	RMSE <sub>interpolation</sub>	0.15 ft (0.05 m)		
RMSE <sub>surface</sub>	0.19 ft (0.06 m)	RMSE <sub>surface</sub>	0.17 ft (0.05 m)	RMSE <sub>total</sub>	0.25 ft (0.76 m)
Mass points (2009)		DTM (1-foot, 2011)		Total Error	
RMSE <sub>z</sub>	0.09 ft (0.03 m)	RMSE <sub>z</sub>	0.07 ft (0.02 m)		
RMSE <sub>interpolation</sub>	na	RMSE <sub>interpolation</sub>	0.12 ft (0.04 m)		
RMSE <sub>surface</sub>	na	RMSE <sub>surface</sub>	0.14 ft (0.04 m)	RMSE <sub>total</sub>	0.17 ft (0.05 m)
Mass points (2009)		TIN (2001)		Total Error	
RMSE <sub>z</sub>	0.09 ft (0.03 m)	RMSE <sub>z</sub>	0.07 ft (0.02 m)		
RMSE <sub>interpolation</sub>	na	RMSE <sub>interpolation</sub>	0.09 ft (0.03 m)		
RMSE <sub>surface</sub>	na	RMSE <sub>surface</sub>	0.12 ft (0.04 m)	RMSE <sub>total</sub>	0.15 ft (0.05 m)

Vertical error in LiDAR data is reported to be more important than error associated with interpolation methods (ASPRS 2004; Hodgson and Bresnahan 2004; Aquillar et al. 2005;

Cvijetonivic et al. 2011). This suggests vertical error contributes more to total error than interpolation error. The reported vertical error for the 2009 and 2011 Catherine Creek LiDAR data is based on GPS check points collected on hard surfaces (e.g., paved and unpaved road). Vertical error for other landscape conditions within the area over which the LiDAR data was acquired are not represented in the error assessment. Whereas vertical error is influenced by topography and land cover (Hodgson et al. 2003, 2004) and point classification (Raber et al. 2002), vertical error was assessed for areas that likely exert the least influence on data quality. The effects of land cover types and topography on classifying terrain points is not represented in the error analysis; no stratified error assessment was provided with the data so reported vertical error is applied globally to the datasets.

The intent of the error analysis was to quantify bounding limits for separating data error and actual change in surface elevation. In applying total error as  $\pm 0.125$  feet to the Catherine Creek difference grid, approximately 26.6% of the study area is within the range of uncertainty (Figure 3). Less than 1% of the study area had height difference values of zero. Surface height difference values over the remainder of the study area (approximately 73.4%) are either greater than 0.125 feet or less than -0.125 feet. This suggests either change in surface elevation has occurred over a large portion of the study area or the error analysis falls short of fully accounting for total error within the datasets.

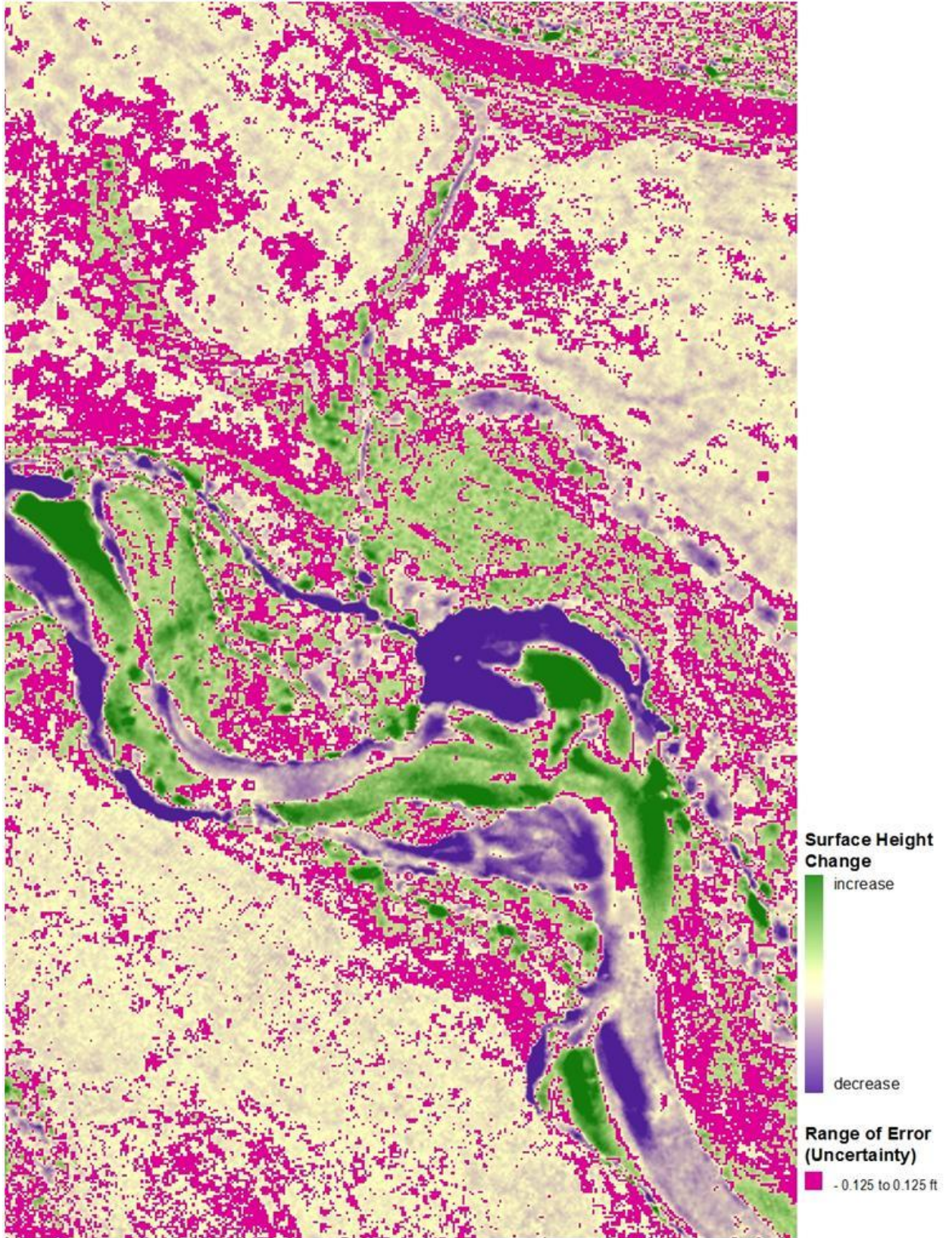


Figure 3. Application of range of uncertainty to surface elevation difference grid.

## Change Detection Approaches

Comparison of Catherine Creek 2009 and 2011 surface elevation values results in difference values indicating some degree of change throughout approximately 99% of the Catherine Creek study area (Figures 3 and 4). Though degree of change can be represented visually, significance of change is not readily apparent and range of uncertainty does not appear to provide a quantitative means to isolate error and identify areas of actual change. Though changes in the active channel migration zone and streambank erosion were detected, changes in vegetation height were also included in height difference results (Figure 4). These results were unexpected from a true DTM. Other mid-values of height difference in the agricultural fields and grassland in the northern and southern portions of the study are further evidence of misclassification errors related to land cover that were not accounted for in total error calculations.

Change detection using Anselin Local Moran I to assess surface elevation difference values clarified the significance of separate height differences through comparison of neighboring values as clusters of values (Figure 5). The statistic identified areas with random distribution of values, patterned clusters of high and low values, and outliers. The results are relative values and vary depending on source data and conceptualization of spatial relationships. Inverse distance assigns larger influence to nearby neighboring feature values than features that are further away. Inverse distance squared is similar to inverse distance except that the slope is sharper and influence drop off more quickly. Mean values for cluster types are similar when comparing the same spatial relationship applied to different data sources (e.g., mean values in Table 3 and Table 5 are similar as are values in Table 4 compared against values in Table 6). Minimum and maximum values vary under these same comparisons primarily because of edge effects in the TIN surface models.

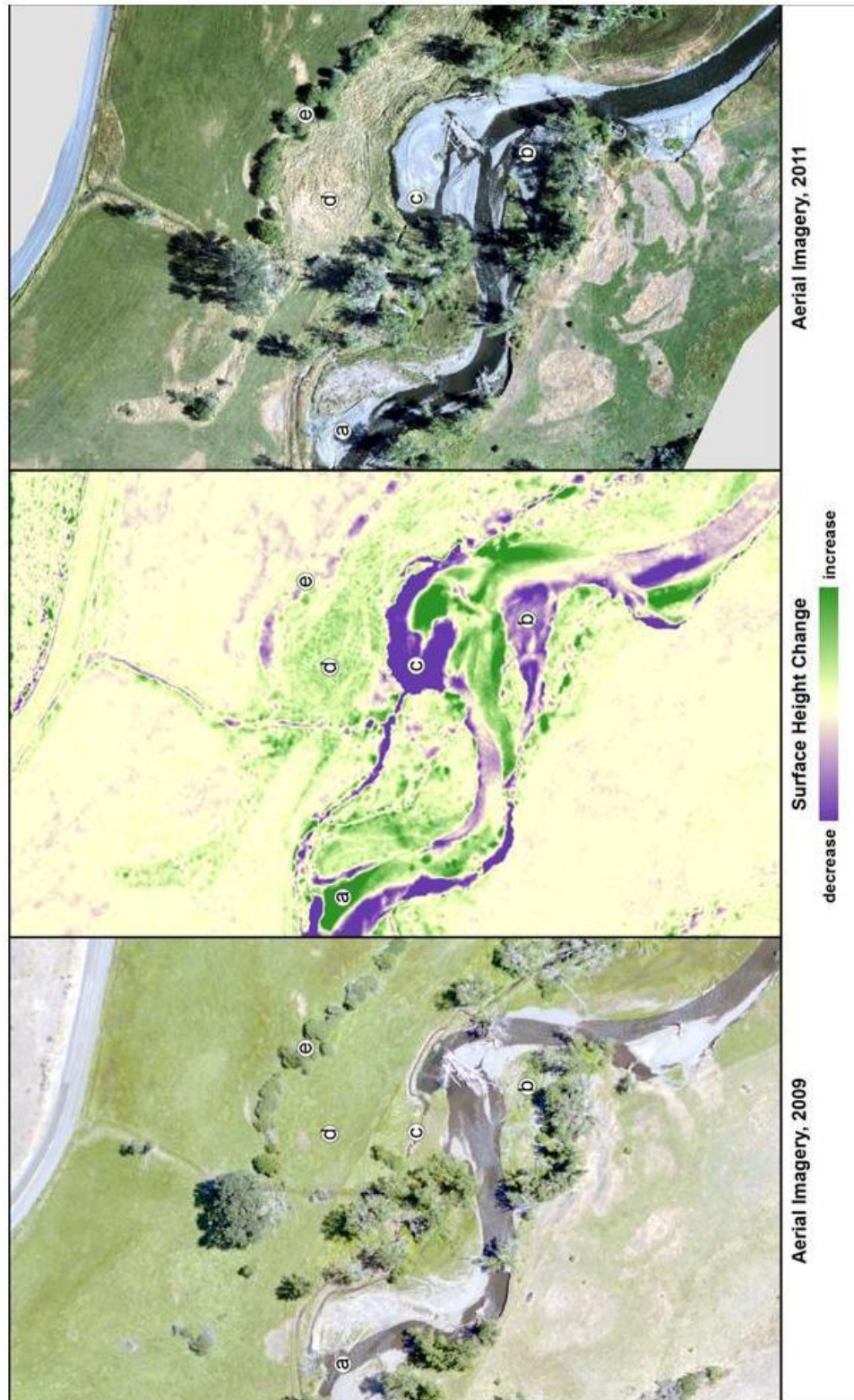
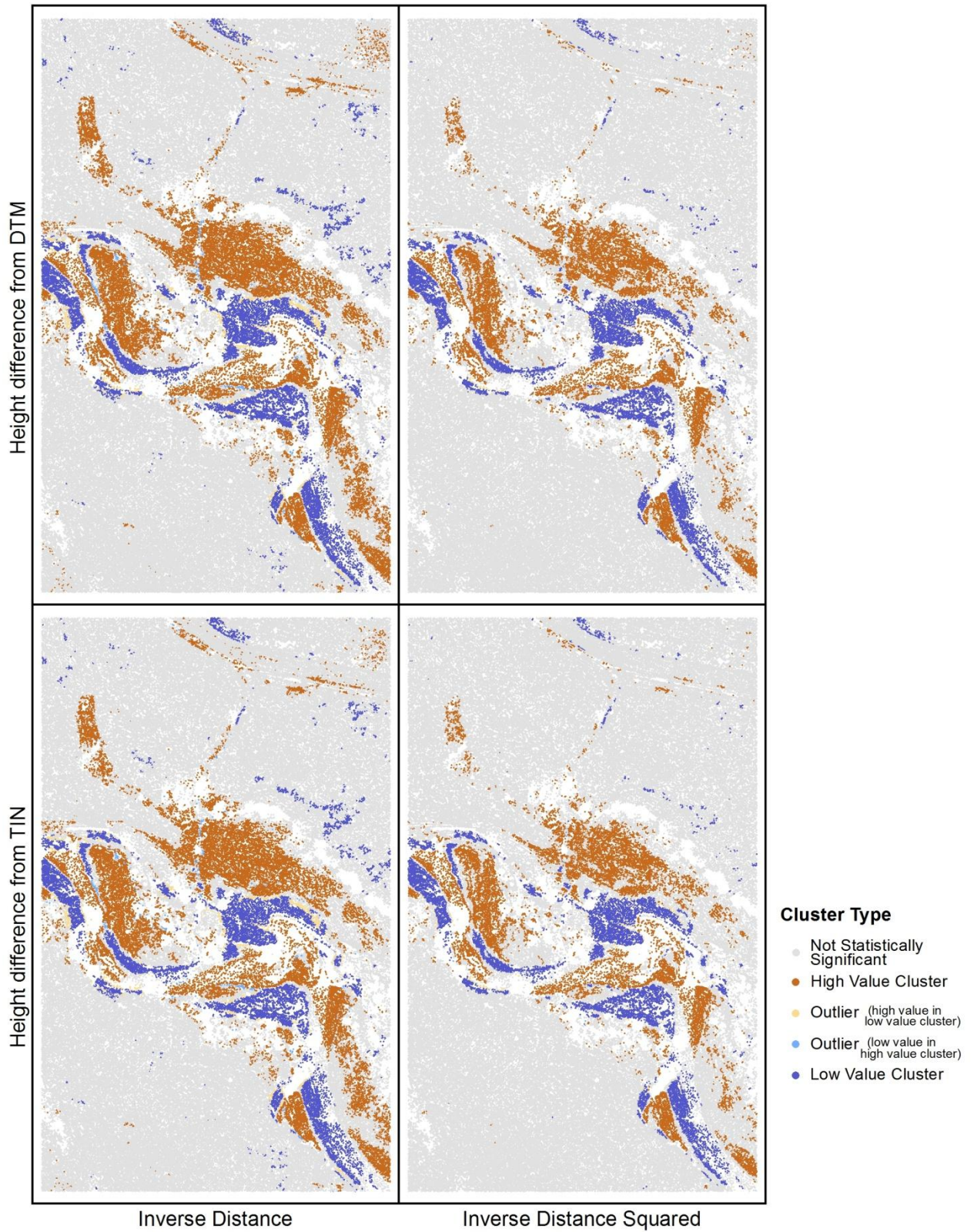


Figure 4. Examples of change detection results for the years between 2009 and 2011: a) deposition of material changing the course of the channel; b) erosion of gravel bar; c) erosion of stream terrace/flood plain; d) height difference of vegetation; e) suggested decrease in canopy height due to LiDAR data classification and/or interpolation error.



**Figure 5. Pattern analysis (Anselin Local Moran I) of surface elevation difference values.**

**Table 3. Height difference values for Anselin Local Moran I Cluster types (mass point to TIN using inverse distance).**

Cluster Type	Height Difference Values		
	Minimum	Maximum	Mean
Not Statistically Significant	-2.30 ft (-0.70 m)	3.68 ft (1.12 m)	-0.17 ft (-0.05 m)
High Values	-0.13 ft (-0.04 m)	6.93 ft (2.11 m)	0.40 ft (0.12 m)
Low Values	-5.95 ft (-1.81 m)	-0.21 ft (-0.06 m)	-1.44 ft (-0.44 m)

**Table 4. Height difference values for Anselin Local Moran I Cluster types (mass point to TIN using inverse distance squared).**

Cluster Type	Height Difference Values		
	Minimum	Maximum	Mean
Not Statistically Significant	-2.69 ft (-0.82 m)	3.68 ft (1.12 m)	-0.16 ft (-0.05 m)
High Values	-0.05 ft (-0.02 m)	6.93 ft (2.11 m)	0.53 ft (0.16 m)
Low Values	-5.95 ft (-1.81 m)	-0.28 ft (-0.09 m)	-1.63 ft (-0.050 m)

**Table 5. Height difference values for Anselin Local Moran I Cluster types (mass point to DTM using inverse distance).**

Cluster Type	Height Difference Values		
	Minimum	Maximum	Mean
Not Statistically Significant	-2.31 ft (-0.70 m)	1.24 ft (0.38 m)	-0.17 ft (-0.05 m)
High Values	-0.08 ft (-0.02 m)	3.36 ft (1.02 m)	0.40 ft (0.12 m)
Low Values	-5.93 ft (-1.81 m)	-0.22 ft (-0.07 m)	-1.45 ft (-0.44 m)

**Table 6. Height difference values for Anselin Local Moran I Cluster types (mass point to DTM using inverse distance squared).**

Cluster Type	Height Difference Values		
	Minimum	Maximum	Mean
Not Statistically Significant	-1.95 ft (-0.59 m)	1.57 ft (0.48 m)	-0.16 ft (-0.05 m)
High Values	-0.04 ft (-0.01 m)	3.36 ft (1.02 m)	0.53 ft (0.16 m)
Low Values	-5.93 ft (-1.81 m)	-0.27 ft (-0.08 m)	-1.64 ft (-0.50 m)

Visual representation of difference values suggest total error, as calculated, did not account for what are probably misclassification errors, particularly in areas of low vegetation (e.g., hay fields, pasture). Total error is likely much higher and not evenly distributed within the datasets. Therefore, even a more accurate and stratified error analysis through which to apply a range of uncertainty to separate height differences by likely error and potential change would still be problematic. Values in statistically insignificant clusters (Tables 3 through 6) indicate a random distribution of height values representing ‘noise’ in the data as opposed to an organized pattern of change. Figure 6 illustrates the range and overlap of height difference values between cluster types. Applying a range of uncertainty would either exclude a wide range of values from consideration (e.g., -0.6 through 0.4 feet) and / or include areas that are reporting anomalously high height difference values that are generalized in error calculations. Discrete values are neither exclusive to any particular cluster type nor specific indicators of change.

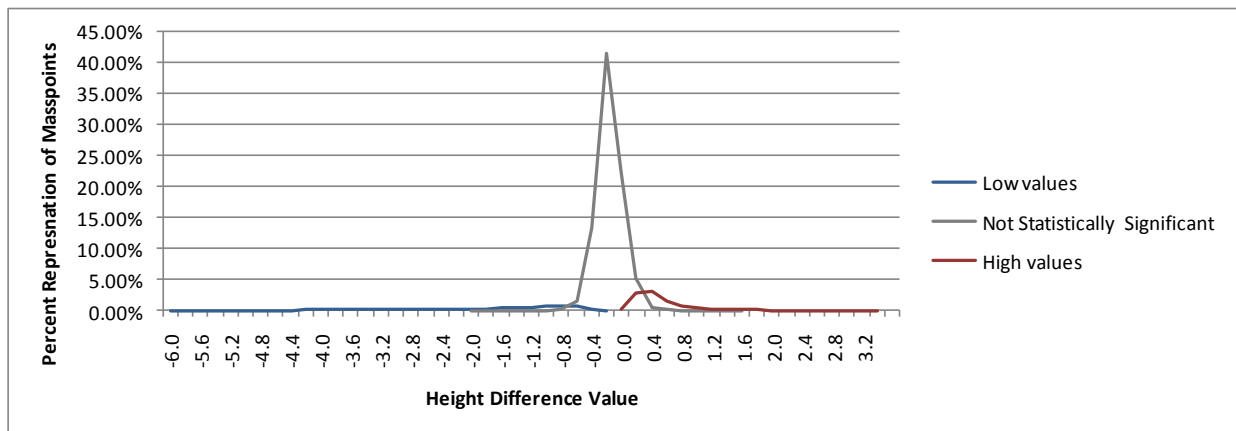


**Figure 6. Frequency distribution of height difference values for Anselin Local Moran I Cluster types.**

The Getis-Ord  $G_i^*$  statistic identifies statistically significant clusters of high or low values, assessing each value within the context of neighboring values. The statistics returns z-scores and p-scores. Z-scores of -1.65 to 1.65 are statistically insignificant and indicative of spatial pattern created by some random process. The corresponding p-values are  $> 0.10$  and carry a confidence level of  $< 90\%$ . Z-scores of  $-1.96 > -1.65$  or  $1.65 > 1.96$  have corresponding p-values of 0.10 to 0.05 and carry a confidence interval of 90% to 95%. The range of z-scores of p-values  $-2.58 > -1.96$  or  $1.96 > 2.58$  relate to p-values of 0.05 to 0.01 having a confidence interval of 95% to 99%. The z-scores  $< -2.58$  or  $> 2.58$  have p-values  $< 0.01$  and confidence of 99% or greater. Applied to the same datasets and spatial relationships as with the Anselin Local Moran I statistics, the Getis-Ord  $G_i^*$  statistic produced similar results (Figure 7).

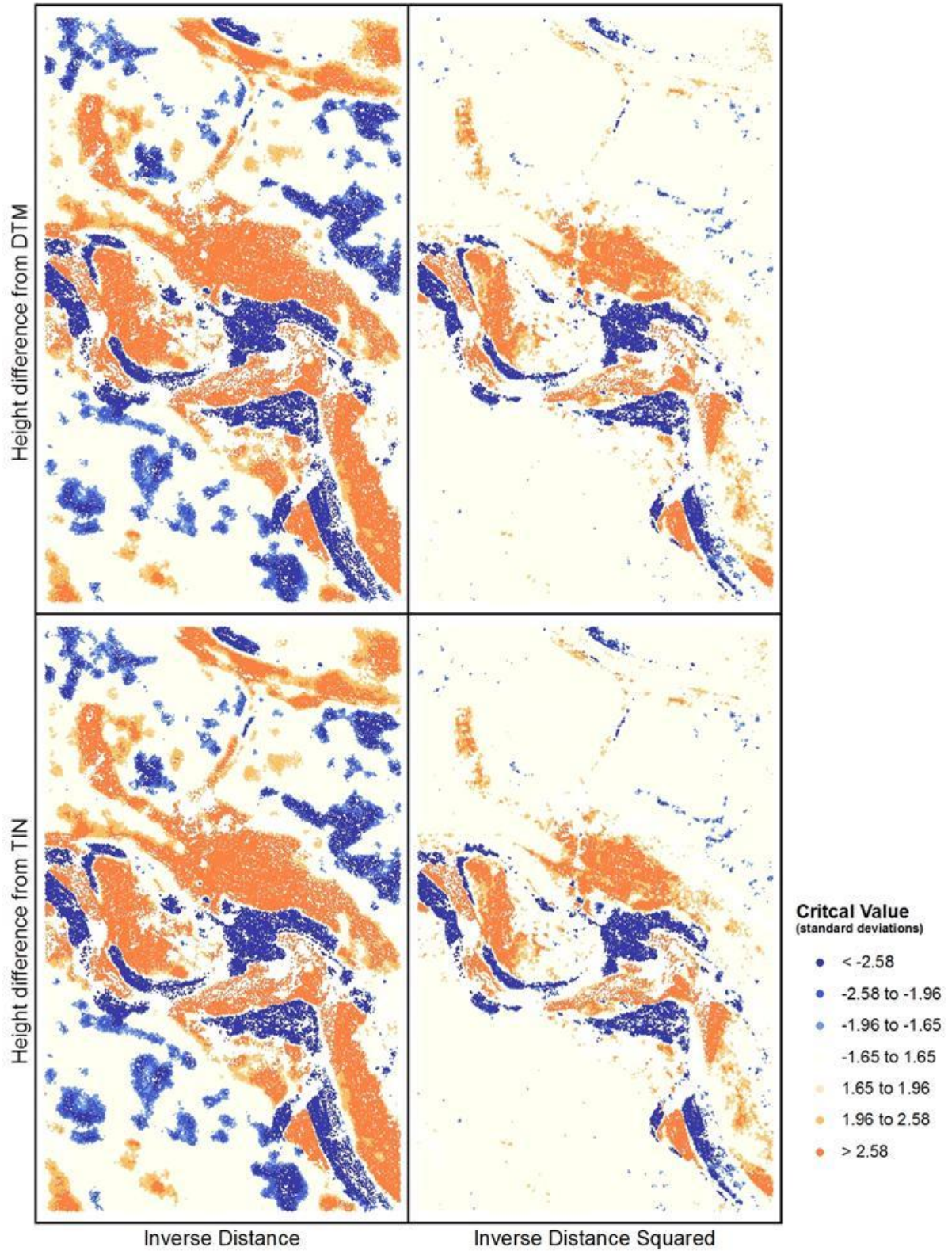
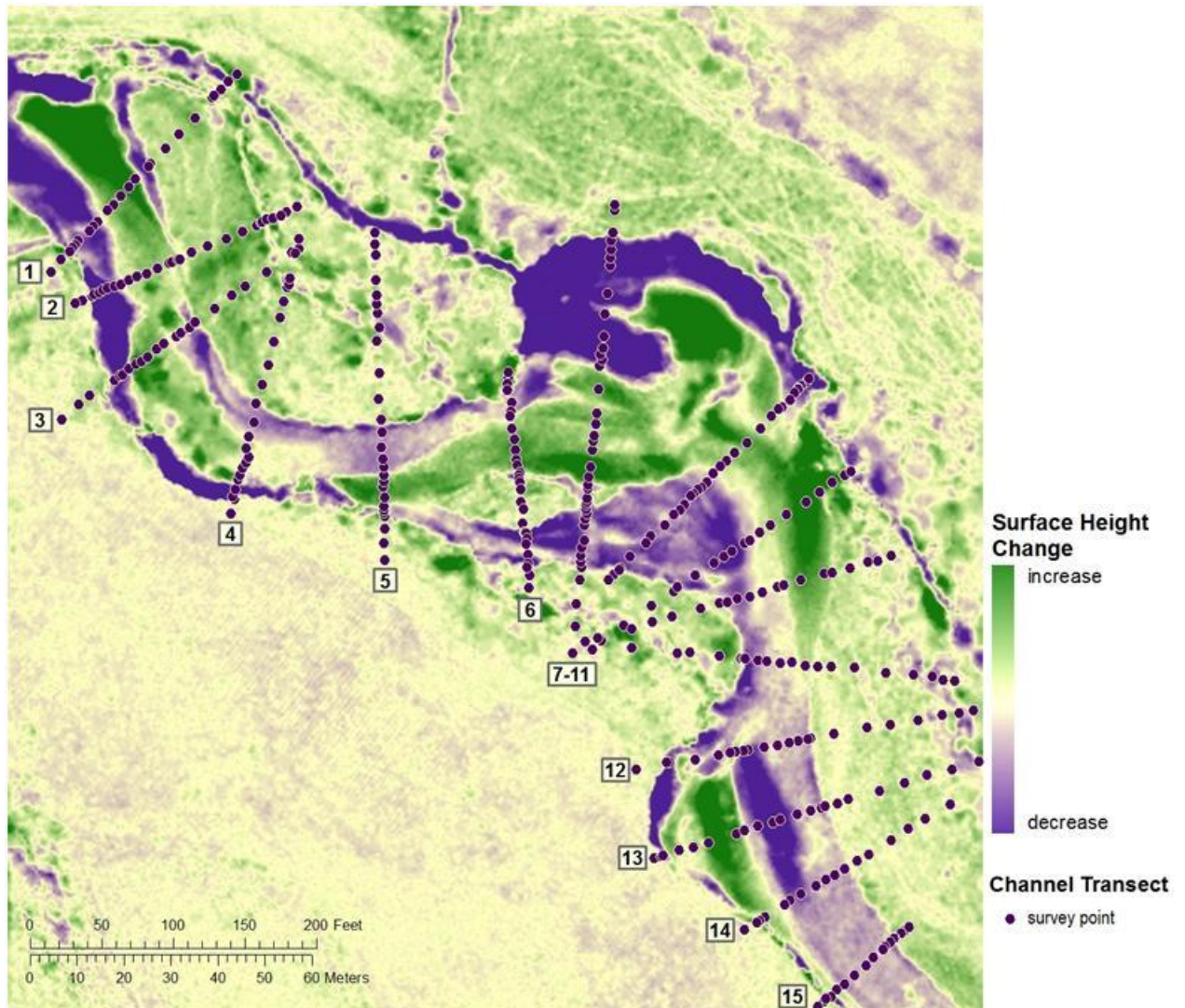


Figure 7. Pattern analysis (Getis-Ord Gi) of surface elevation difference values.

Survey data collected as cross sections of the Catherine Creek stream channel, provides the means to assess terrain representation of the 2011 Catherine Creek LiDAR dataset and estimate surface changes from the 2009 dataset. The survey transects represent varying degrees of change in the Catherine Creek surface-to-surface difference grid (Figure 8).



**Figure 8. Channel cross-section survey transects with 2009/2011 difference grid.**

Elevation values from the 2009 and 2011 Catherine Creek DTMs coincident with survey points provide comparative cross-sections (Figures 9 through 23). Survey field notes and aerial imagery were used to associate the survey points to vegetated bank, gravel bar, and watered channel (as green, orange, and blue lines, respectively) for 2009 and 2011.

Horizontal lines at the top of the charts describe extents of 2009 features and lines at the bottom of each chart describe feature extents for 2011.

Elevation values for the 2011 DTM and 2011 field survey are generally in agreement (for example, Figures 9, 10, 11, 14, 15, 17, and 18) though rarely exact. Apart from error identified in the LiDAR datasets and interpolated surface model the survey data is not without error, as is particularly obvious in stations 191.23 through 203.47 of transect 8 (Figure 16). Otherwise, the difference in representation of the stream channel is the result of sampling approach. The LiDAR pulses reflect off the surface of the water whereas the channel bottom was sampled in the survey.

Likewise, the 2009 data generally agrees with the 2011 LiDAR and survey data in areas along transects where change had not occurred. Elevation differences where change had occurred reflects the degree of change; high degree of change for streambank to stream channel transition and more moderate degree of change for gravel bar to stream channel or stream channel to gravel bar transitions. This is reflected in the surface-to-surface difference grid (Figure 8). However, as it was shown that in evaluating change on the basis of absolute values for height differences in surface-to-surface comparisons, the range in elevation difference in the transects is equally unreliable. Error between the 2009 and 2011 data, independent datasets, is evident in areas where change had not occurred; particularly in areas of low vegetation or water surface (see transect 5 stations 60.78-79.75, 164.88-215.81 and transect 11 stations 200.18-230.09; Figure 13 and Figure 19, respectively). Comparison of transect 14 elevation differences for stations 47.61-83.31 (Figure 22) against critical values generated by the Getis-Ord  $G_i^*$  statistic (Figure 24), shows no change detection despite difference in elevation values of nearly 1-foot. The statistic did not detect a process-related distribution of elevation difference values, but rather a random distribution of values.

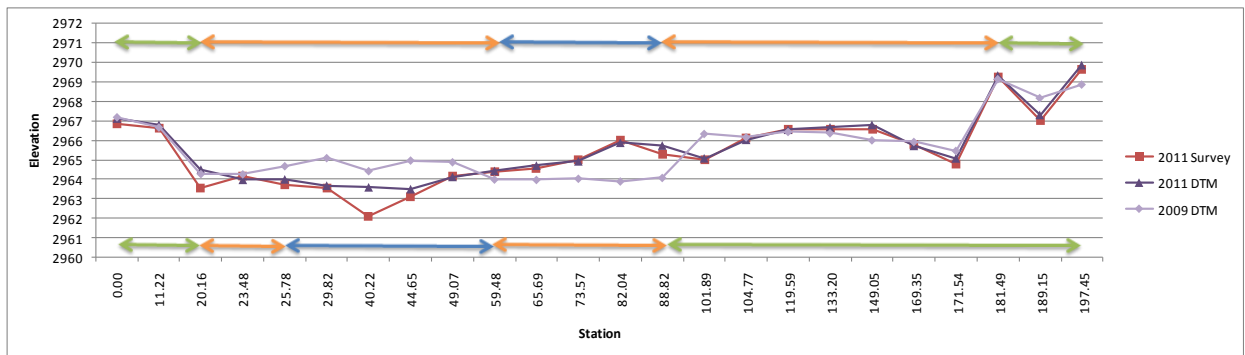


**Figure 9. Line graph of channel cross sections at transect 1.**

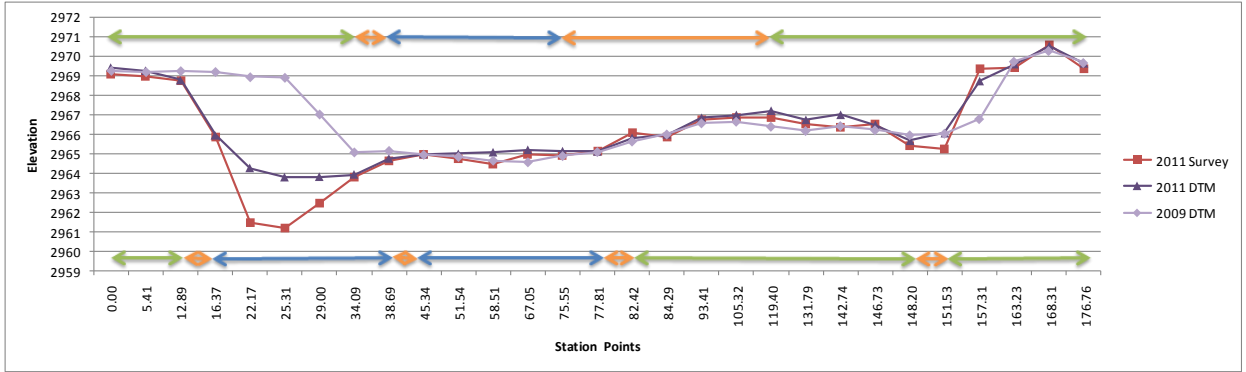


Figure 10. Line graph of channel cross sections at transect 2.

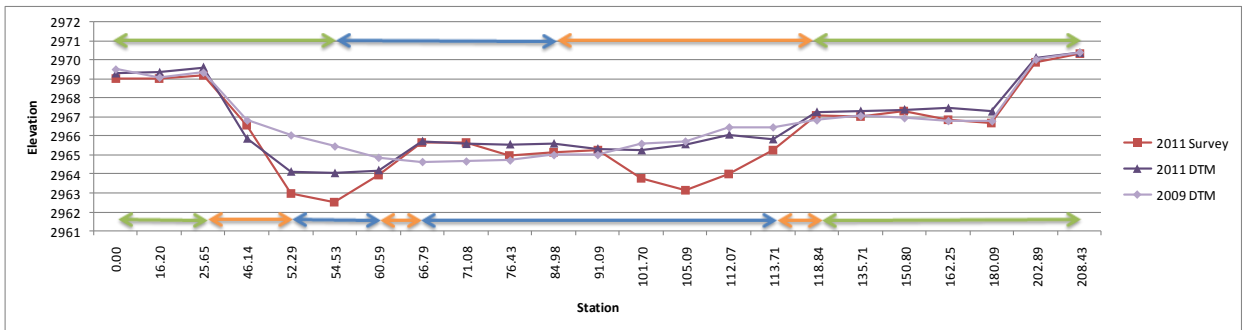


Figure 11. Line graph of channel cross sections at transect 3.

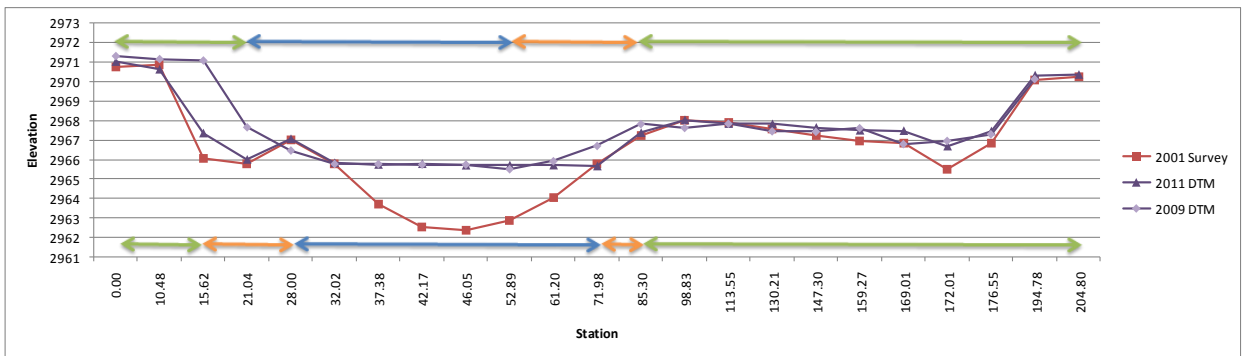


Figure 12. Line graph of channel cross sections at transect 4.

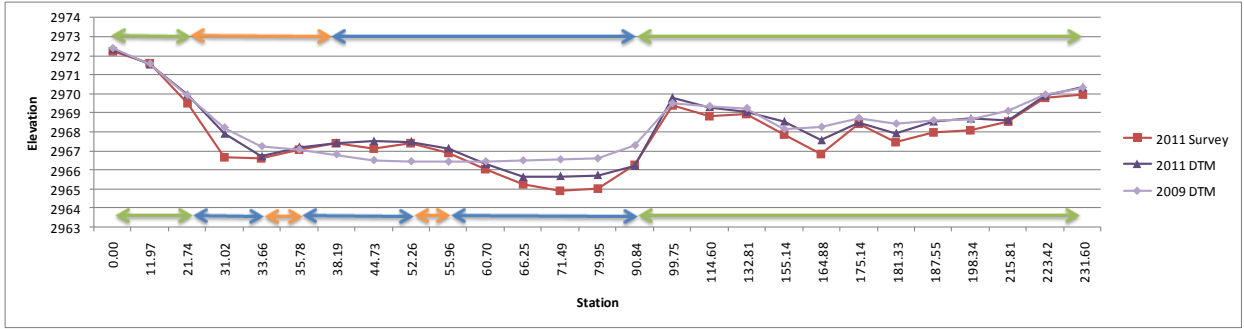


Figure 13. Line graph of channel cross sections at transect 5.

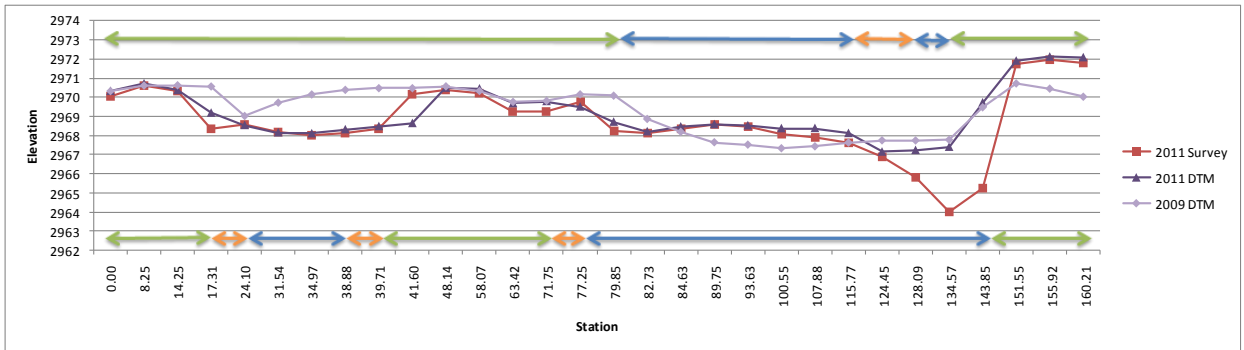


Figure 14. Line graph of channel cross sections at transect 6.

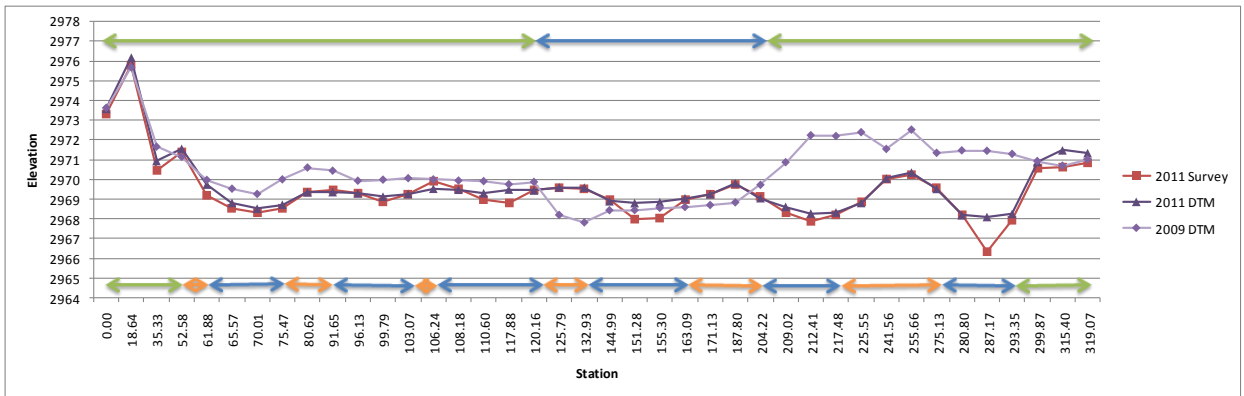


Figure 15. Line graph of channel cross section at transect 7.

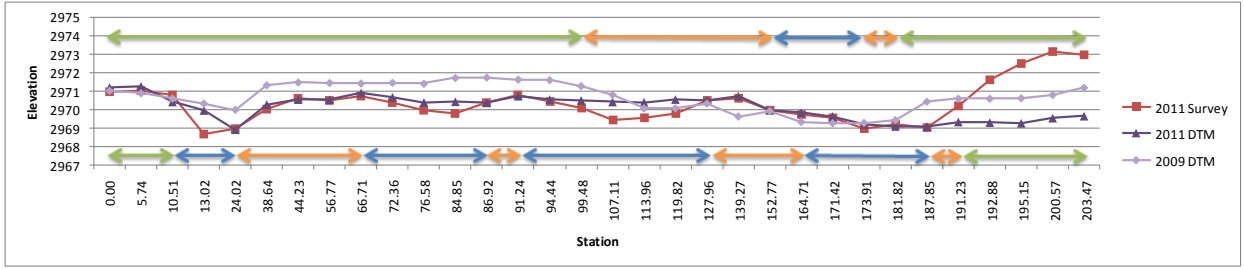


Figure 16. Line graph of channel cross section at transect 8.

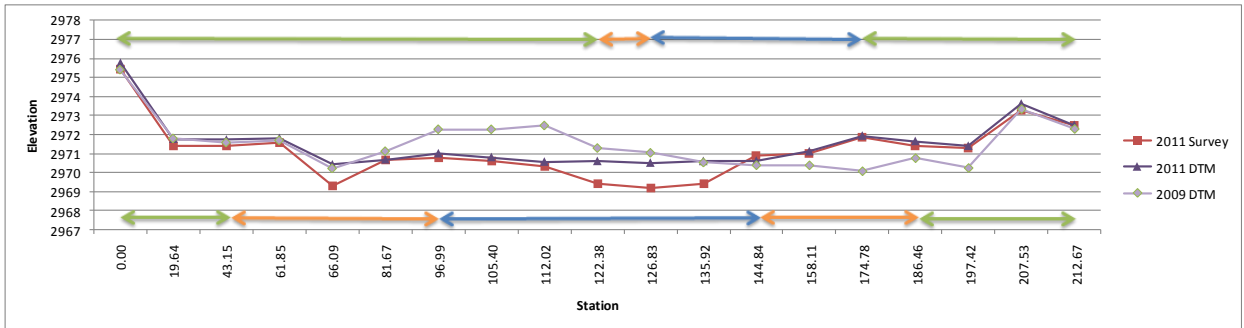


Figure 17. Line graph of channel cross section at transect 9.

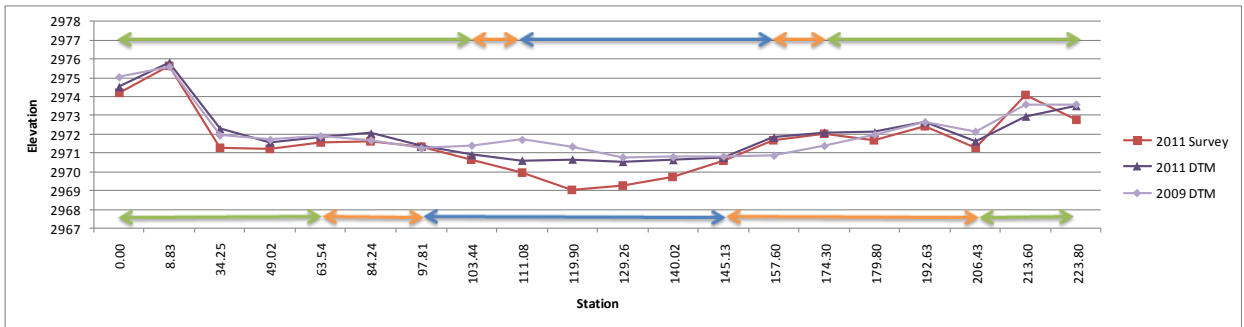


Figure 18. Line graph of channel cross section at transect 10.

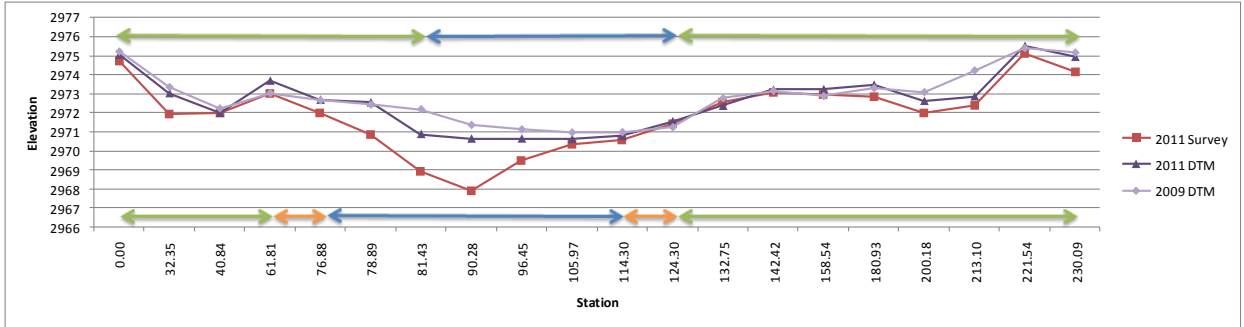


Figure 19. Line graph of channel cross section at transect 11.

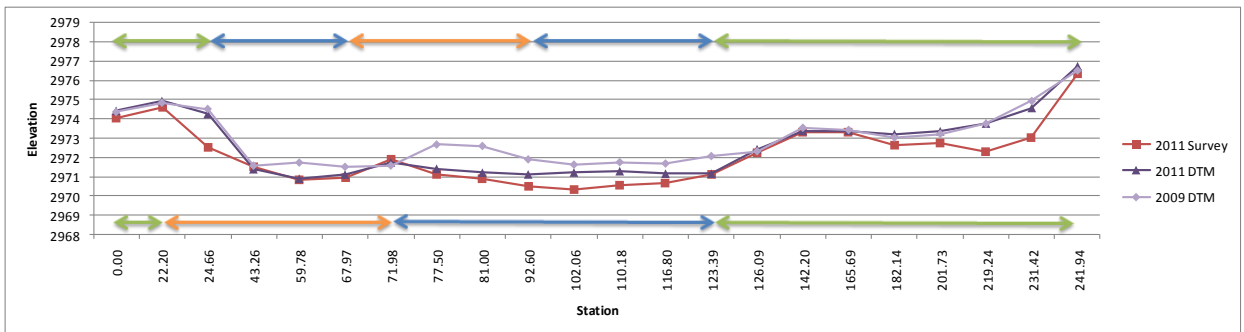


Figure 20. Line graph of channel cross section at transect 12.

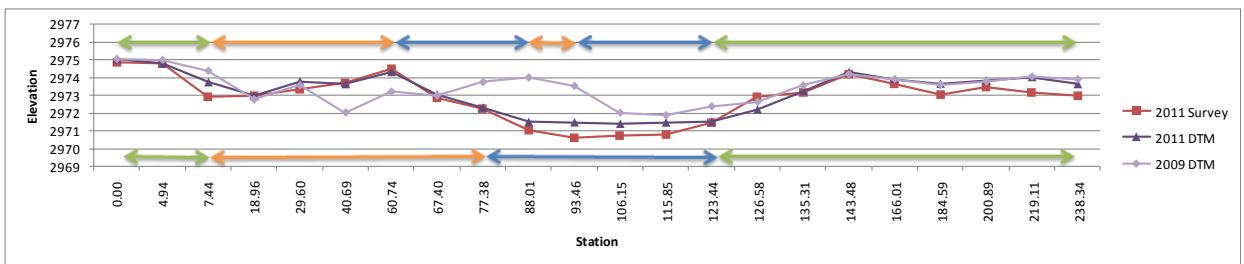
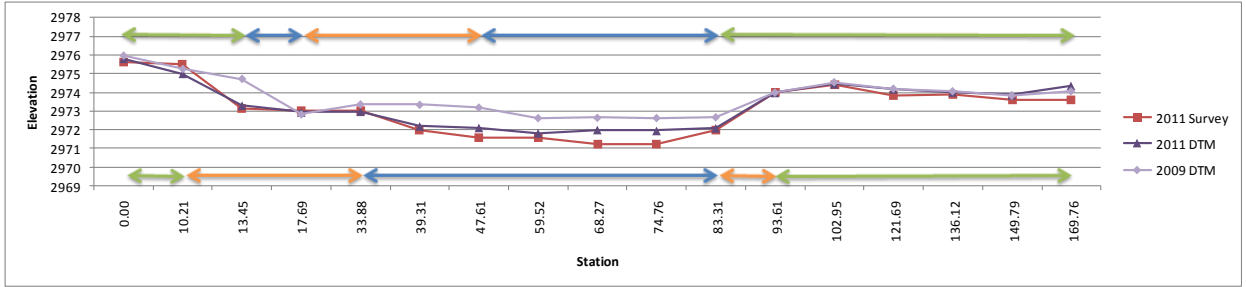
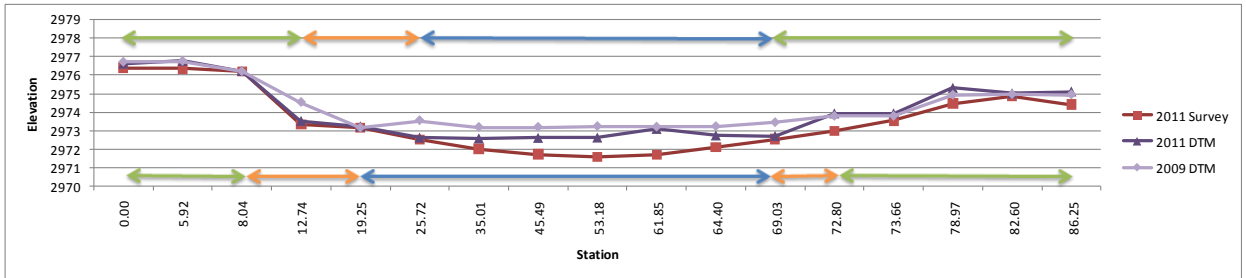


Figure 21. Line graph of channel cross section at transect 13.



**Figure 22. Line graph of channel cross section at transect 14.**



**Figure 23. Line graph of channel cross section at transect 15.**

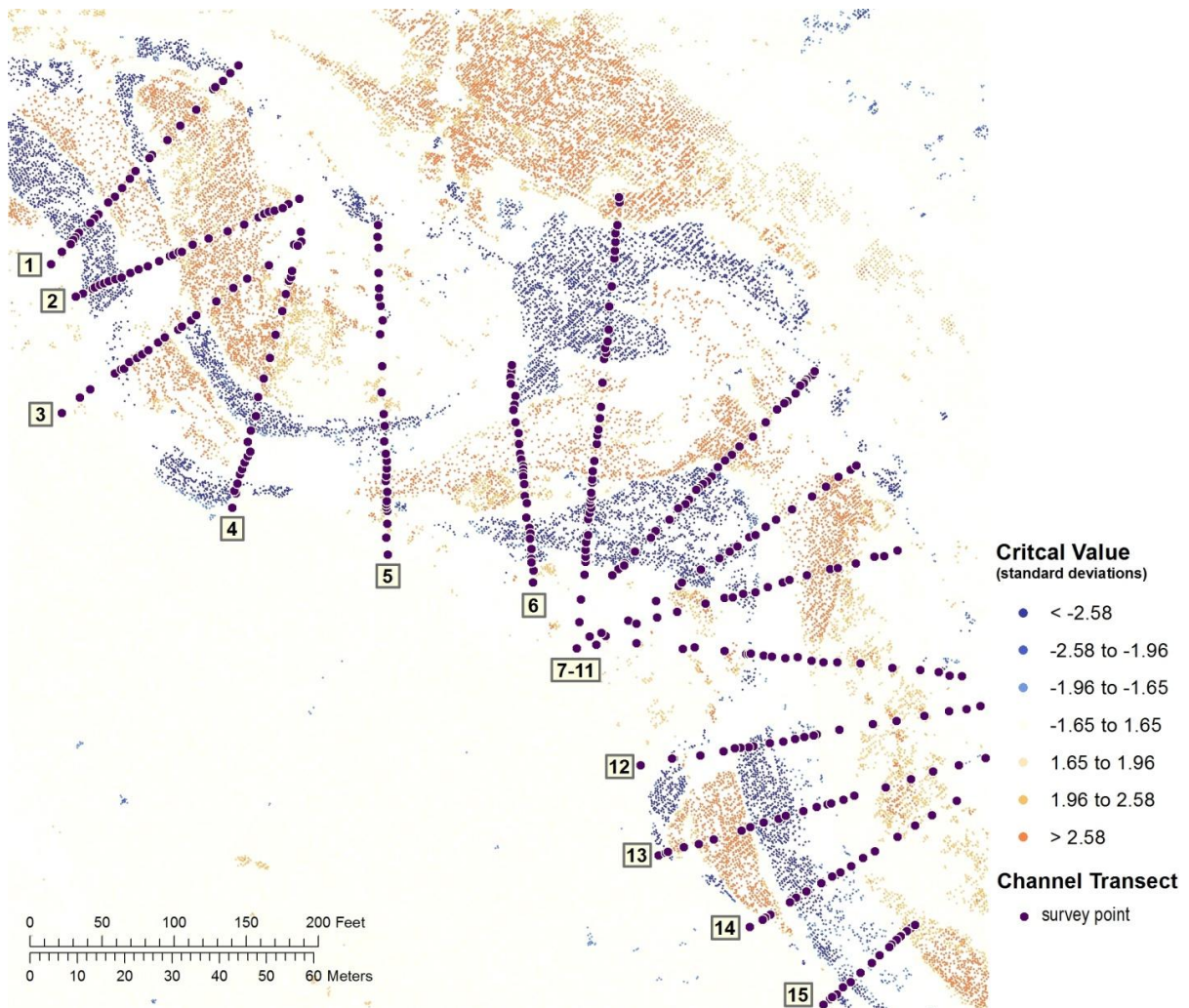


**Figure 24. Channel profile survey transects with Getis-Ord  $G_i^*$  results for 2009 points and 2011 1-foot DTM.**

Change detection results for the Lake Walcott datasets reported suspect height difference values for high-value and low-value statistically significant point clusters (Tables 7 through 10). For example, an increase in elevation for sites within Tile 03 was never less than 3.17 feet and nearly approached 12.5 feet (Table 7). No evidence of disturbance was identified through visual inspection of aerial imagery for those sites where change was reported. Overall, visual inspection of aerial imagery confirmed that increases or decreases in elevation in the range of 60 feet within the Lake Walcott study area are unrealistic. The frequency of height differences greater than 4 feet within high value point clusters suggests systematic error in either one or both of the Lake Walcott datasets (Table 11). Metadata for each of the datasets was insufficient for evaluating the data; the error was not identified.

**Table 7. Height difference values for Anselin Local Moran I Cluster types (Lake Walcott, Tile 03).**

Cluster Type	Height Difference Values		
	Minimum	Maximum	Mean
Not Statistically Significant	-0.88 ft (-0.27 m)	5.70 ft (1.74 m)	3.09 ft (0.94 m)
High Values	3.17 ft (0.97 m)	12.41 ft (3.78 m)	4.08 ft (1.24 m)
Low Values	-14.73 ft (-4.49 m)	2.94 ft (0.90 m)	1.64 ft (0.50 m)

**Table 8. Height difference values for Anselin Local Moran I Cluster types (Lake Walcott, Tile 05).**

Cluster Type	Height Difference Values		
	Minimum	Maximum	Mean
Not Statistically Significant	-5.33 ft (-1.62 m)	10.44 ft (3.18 m)	2.95 ft (0.90 m)
High Values	2.96 ft (0.90 m)	42.91 ft (13.08 m)	3.92 ft (1.94 m)
Low Values	-14.94 ft (-4.55 m)	2.88 ft (0.88 m)	1.84 ft (0.56 m)

**Table 9. Height difference values for Anselin Local Moran I Cluster types (Lake Walcott, Tile 07).**

Cluster Type	Height Difference Values		
	Minimum	Maximum	Mean
Not Statistically Significant	-9.00 ft (-2.74 m)	10.03 ft (3.06 m)	3.04 ft (0.93 m)
High Values	3.04 ft (0.94 m)	67.30 ft (20.51 m)	4.45 ft (1.36 m)
Low Values	-26.69 ft (-8.14 m)	2.30 ft (0.70 m)	1.91 ft (0.58 m)

**Table 10. Height difference values for Anselin Local Moran I Cluster types (Lake Walcott, Tile 10).**

Cluster Type	Height Difference Values		
	Minimum	Maximum	Mean
Not Statistically Significant	-17.98 ft (-5.48 m)	8.77 ft (2.67 m)	3.18 ft (0.97 m)
High Values	3.23 ft (0.98 m)	68.10 ft (20.76 m)	4.21 ft (1.28 m)
Low Values	-62.26 ft (-18.98 m)	3.12 ft (0.95 m)	1.68 ft (0.51 m)

**Table 11. Frequency of Probable Error in Height Difference Values for Lake Walcott Tiles**

<b>Tile</b>	<b>High Values &gt; 4 ft</b>	<b>Low Values &lt; -4 ft</b>
03	40.05%	1.48%
05	22.21%	0.54%
07	28.26%	1.23%
10	31.44%	2.82%

## **Discussion**

Change detection, based on absolute measures of change in temporally discrete surface elevation values, is problematic. It is difficult to calculate and compensate for total error in the LiDAR associated with data acquisition and processing. Whereas system error can be minimized using universally applied correction, vertical error is influenced by numerous factors that are asymmetrically represented within the landscape. It is difficult to compute and apply stratified error to identify spatially explicit uncertainty in surface difference values. Furthermore, with broad ranges of uncertainty values, some areas of detected change are likely to be excluded from consideration; minimizing the precision to which a change analysis can be performed.

Applying spatial statistics to assess neighboring values and report relative significance of point clusters appears to show promise in conducting analyses of elevation changes between temporally discrete LiDAR datasets. The most critical factor affecting results appears to be data resolution in terms of post-spacing. Considering the deviation in terrain representation between independent datasets, higher point density increases likelihood of near-coincident mass points and minimize effects of the random sampling of surface values.

Timing of data acquisition is important with respect to not only capturing the change element of interest but excluding confounding factors. A comparison of the Catherine Creek datasets, acquired in August 12 through 15, 2009, and September 29, 2011, identified an agricultural area as a site of change on the basis of difference in height of grasses. The difference was most likely due to agricultural practices but does demonstrate that seasonal variation in vegetation could confound or even mask change detection results.

Aerial imagery, acquired in conjunction with elevation data is critical in confirming interpretation of change detection results. A change in elevation may indicate that a disturbance may have occurred; visual inspection of aerial imagery, for those periods for which change detection is being conducted, may reveal what disturbance (if any) did occur. True color imagery had been acquired with the LiDAR data for both the Catherine Creek and Lake Walcott study areas. Color- infrared imagery (i.e., 4-band imagery) is readily available and should be considered for integration into the proposed change detection methodology.

Further research to investigate detection of off-road vehicular (ORV) should be considered. No examples were present in the Catherine Creek study area and post-spacing was far too gross to assess the increase in ORV use within the Lake Walcott study area between 2003 and 2011. Assuming ORVs will impact vegetation cover, an impact area the width of even an all-terrain vehicle may be detectable using the proposed methodology.

The feasibility of using LiDAR as a monitoring tool based on cost of acquisition was not assessed. Cost-benefit should consider field hours to monitor sites, impacts of visits to sites, and resource value.

## References

### Parenthetical Reference

### Bibliographic Citation

Aguilar et al.. 2010

Aguilar, F.J., J.P. Mills, J. Delgado, M.A. Aguilar, J.G. Negreiros, and J.L. Perez. 2010. Modeling vertical error in LiDAR-derived digital elevation models. *ISPRS Journal of Photogrammetric and Remote Sensing*, 65:103-110.

Aguilar, Aguera, and Carvjal 2005

Aguilar, F.J., F. Aguera, M.A. Aguilar, and F. Carvjal. 2005. Effects of terrain morphology, sampling density, and interpolation methods on grid DEM accuracy. *Photogrammetric Engineering & Remote Sensing*, 71(7):805-816.

ASPRS 2004

ASPRS. 2004. *ASPRS Guideline Vertical Accuracy Reporting for Lidar Data V1.0*. American Society of Photogrammetry and Remote Sensing, Bethesda, MD.

Cebecauer, Hofierka, and Suri 2002

Cebecauer, T., J. Hofierka, and M. Suri. 2002. Processing digital terrain models by regularized spline with tension: tuning interpolation parameters for different input datasets. In *Proceedings of the Open Sources GIS – GRASS users conference*, September 11-13, Trento, Italy.

Cvijentinovic et al.. 2011

Cvijentinovic, Z., D. Mihajlovic, M. Vojinovic, and M. Mitrovic. 2011. Terrain surface modeling using triangular spline patches. In *Proceedings of the International Conference and XXIV Meeting of Serbian Surveyors*, June 24-26, Kladovo-Djerdap upon Danube, Serbia.

FGDC 1998

Federal Geographic Data Committee. FGDC-STD-001-1998. Content standard for digital geospatial metadata (revised June 1998). Federal Geographic Data Committee. Washington, D.C.

**Parenthetical Reference****Bibliographic Citation**

Gallay, Lloyd, and  
McKinley 2012

Gallay, M., C. Lloyd, and J. McKinley. 2012. Optimal interpolation of airborne laser scanner data for fine-scale DEM validation purposes. In Proceedings of Symposium GIS Ostrava 2012 – Surface models for geosciences, January 23-25, Ostrava, Czech Republic.

Guo et al. 2010

Guo, Q, W. Li, H. Yu, and O. Alvarez. 2010. Effects of topographic variability and lidar sampling density on several DEM interpolation methods. *Photogrammetric Engineering & Remote Sensing*, 76(6):1-12.

Hodgson and Bresnahan  
2004

Hodgson, M.E., and P. Bresnahan. 2004. Accuracy of airborne lidar-derived elevation: empirical assessment and error budget. *Photogrammetric Engineering & Remote Sensing*, 70(3):331-339.

Kohavi 1995

Kohavi, R. 1995. A study of cross-validation and bootstrap for accuracy estimation and model selection. *Proceedings: International Joint Conference on Artificial Intelligence*.

McGwire 1996

McGwire, K.C. 1996. Cross-validated Assessment of geometric accuracy. *Photogrammetric Engineering & Remote Sensing*, 62(10):1179-1187.

Raber 2002

Raber, G.T., J. R. Jensen, S. R. Schill, and K. Schuckman. 2002. Creation of digital terrain models using an adaptive lidar vegetation point removal process. *Photogrammetric Engineering & Remote Sensing*, 68(12):1307-1315.